# Removal of EOG Artifacts From Single Channel EEG Signals Using Combined Singular Spectrum Analysis and Adaptive Noise Canceler

Ajay Kumar Maddirala and Rafi Ahamed Shaik, *Member, IEEE*

***Abstract*— The electroencephalogram (EEG) signals represent the electrical activity of the brain. In applications, such as brain–computer interface (BCI), features of the EEG signals are used to control the devices. However, while recording, EEG signals often contaminated by electrooculogram (EOG) artifacts; such artifacts degrade the performance of the BCI. In this paper, we proposed a new technique using singular spectrum analysis (SSA) and adaptive noise canceler (ANC) to remove the EOG artifact from the contaminated EEG signal. In this technique, first, we proposed a novel grouping technique for SSA to construct the reference signal (EOG) for ANC. Later, using the extracted reference signal, the adaptive filter was employed to remove EOG artifact from the contaminated EEG signal. To quantify the performance of the proposed technique, we carried out simulations on synthetic and real-life EEG signals. In terms of relative root mean square error and mean absolute error, the proposed SSA-ANC method outperforms the existing techniques.**

***Index Terms*— Electroencephalogram (EEG), electrooculogram (EOG), singular spectrum analysis (SSA), singular value decomposition (SVD), adaptive noise canceler (ANC).**

## I. Introduction

THE electroencephalogram (EEG) signals measured by keeping electrodes over the scalp represents the electrical activity of the brain. In practice, while recording, EEG signals often contaminated by electrooculogram (EOG) artifact caused by eye blink or movement. In applications such as brain computer interface (BCI), the features of the EEG signals are used as a commands to control the devices and hence the presence of such artifacts may degrade the performance of the BCI system [1]. One possible solution in reducing EOG artifact in EEG signals is instructing the subject to make no eye blink or movement. However, such instruction may impose secondary task on the subject. Hence, removal of eye artifact plays vital role in EEG signal analysis.

The regression-based techniques both in time and frequency domain have been proposed to remove EOG artifact from the EEG signal recorded for evoked potential (EP) studies [2], [3]. In these techniques, the average transfer coefficients between the EOG and each EEG channels are estimated using calibrated EEG data obtained in various conditions. In practice, as the EEG and EOG signals are non-stationary signals, the average transfer coefficients are inadequate to remove EOG artifact from the real-time EEG signals. Hence, there is a need of adaptive filters [4] to track such non-stationary signal variations is highly desirable.

Adaptive noise cancelers (ANCs) [5] are widely used to remove artifacts from the biomedical signals [6]–[9]. However, these techniques assumes that the reference signal for ANC is available. In [10], ANC has been used along with the independent component analysis (ICA) to identify the independent components representing the EOG artifact. The reference signals for ANC is obtained by employing the ICA on the EEG signals recorded at electrodes closet to the eye ($F_{p_1}$ or $F_{p_2}$). However, this technique is applicable for analysis of multichannel EEG signals and hence cannot applicable for portable devices.

The removal of high amplitude EOG artifact from single channel EEG signal using local singular spectrum analysis (SSA) [11], [12], has been proposed in [13] and [14]. In this technique, the feature vectors of the embedded matrix, obtained by arranging delayed version of original signal, are clustered by $k$-means [15] algorithm. The eigenvalues and eigenvectors of the covariance matrix of each cluster are computed using singular value decomposition (SVD). In order to estimate EOG artifact, the minimum description length (MDL) [16] criteria is used, which gives the information regarding the dimension of signal subspace or the number of eigenvectors needed to estimate the EOG signal. However, for reliable estimation of dimension of signal subspace, there should be enough magnitude difference or gap between the eigenvalues, representing EOG and EEG signals [13]. In order to remove artifacts from frontal EEG signals, where the magnitude of EOG artifact in the EEG signal is high, the local SSA exhibits good performance in removing EOG artifact efficiently. Whereas in applications such as BCI motor imagery task, there will be power differences in the EEG $\alpha$ $(8-12Hz)$ and $\beta$ $(18-26Hz)$ rhythms [17]. To capture such useful information, the EEG signals are often recorded at electrode positions $C_3$ and $C_4$ [18]. As these electrodes are far from the eye, which is a source of generating EOG artifact, the magnitude of EOG component present in the EEG signal is small compared with the signal recorded from the frontal EEG electrodes. As the magnitude of EOG component in EEG signal is small, there will be no such gap or magnitude difference in the eigenvalues, representing the EOG and EEG signals,

Manuscript received November 15, 2015; revised February 17, 2016; accepted April 15, 2016. Date of publication April 28, 2016; date of current version November 4, 2016. The associate editor coordinating the review of this paper and approving it for publication was Prof. Daniela De Venuto.

The authors are with the Department of Electronics and Electrical Engineering, Indian Institute of Technology, Guwahati 781039, India (e-mail: a.maddirala@iitg.ernet.in; rafiahamed@iitg.ernet.in).

Digital Object Identifier 10.1109/JSEN.2016.2560219

1558-1748 © 2016 IEEE. Personal use is permitted, but republication/redistribution requires IEEE permission.
See http://www.ieee.org/publications_standards/publications/rights/index.html for more information.

Authorized licensed use limited to: Universita degli Studi di Roma La Sapienza. Downloaded on October 07,2021 at 15:30:23 UTC from IEEE Xplore. Restrictions apply.

and hence the MDL criteria may fail in estimating appropriate dimension of the signal subspace. Hence, the corrected EEG signal still may have the remnants of the EOG artifact.

Recently in [19], adaptive line enhancer (ALE) based on the SSA has been proposed to separate electrocardiogram (ECG) from the electromyogram (EMG) signals by exploiting the periodicity of ECG signal. Unlike ANC, where two separate inputs are needed to filter out the artifact, here, by exploiting the periodicity of the artifact present in the contaminated signal and its delayed version, the ALE removes the artifact signal. In general, this delay is set based on the periodicity of the artifact present in the contaminated signal. However, as the EEG and EOG signals are non-stationary signals, such technique exhibits poor performance in removing the EOG artifact from the EEG signal.

More recently, a combined use of discrete wavelet transform (DWT) and ANC, namely DWT-ANC, has been proposed in [20] to remove EOG artifact from EEG signals. In this technique, firstly, the DWT is used to construct the reference signal, *i.e*. EOG, from the contaminated EEG signal and is applied to reference input of the ANC. Finally, the ANC removes the EOG artifact from the contaminated EEG signal by changing the filter coefficients based on the adaptive algorithm. However, the performance of this technique mainly depends on how good is the estimated reference signal, which in turn depends on the selection of wavelet function and the number of decomposition levels. However, the selection of wavelet function and decomposition levels depends on the morphology of the EOG artifact and its frequency spectrum.

In order to overcome these limitations, in this paper, we proposed a combined SSA and ANC, named as SSA-ANC, to remove EOG artifact from the EEG signal. SSA is a subspace based technique used to decompose given signal into trend, oscillating and noise components and is often used in the analysis of climatic and geophysics time series [11], [12]. Like DWT-ANC, the reference signal *i.e*. EOG signal is estimated from the contaminated EEG signal by SSA, and is given to the reference input of the ANC. While estimating the reference EOG signal, unlike local SSA, where the magnitudes of eigenvalues are used in estimating the signal subspace, we proposed a novel grouping technique using local mobility of the eigenvectors in estimating the EOG signal subspace. As the EOG signal is reconstructed based on heuristic approach (*i.e*., threshold defined by the user), EOG artifact is not efficiently reconstructed. Hence, direct subtraction of estimated EOG artifact from the contaminated may retain some of the EOG components. To remove the remnants of the EOG artifact, SSA has to be combined with ANC. Finally, the ANC removes the EOG artifact by changing the filter coefficients based on the adaptive algorithm. Simulation results show that proposed SSA-ANC technique exhibits better performance than the DWT-ANC.

This paper is organized as follows: Section II provides a detailed introduction about ANC and DWT-ANC. The proposed SSA-ANC technique and the key steps are explained in Section III. The discussion of simulation results and conclusion are outlined in Section IV and V, respectively.

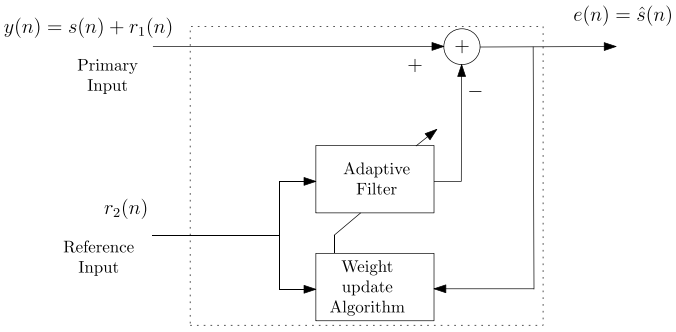


Fig. 1. Block diagram of adaptive noise canceler (ANC).

## II. Techniques

### A. Adaptive Noise Canceler

The adaptive noise canceler as shown in Fig. 1, basically consists of filtering and weight updating blocks. The weights of the adaptive filter can be updated using either least mean square (LMS) or recursive least square (RLS) algorithms [4]. In this paper, we have employed RLS because of the fact that the filter coefficients using this algorithm are tuned to optimum values in a less number of iterations, *i.e*. fast convergence. Let the tap input vector and the filter coefficient vector of $P$-tap adaptive filter at time instant $n$ is denoted as $\mathbf{r}_2(n) = [r_2(n), r_2(n-1), \ldots, r_2(n-P+1)]^T$ and $\mathbf{w}(n) = [w_1(n), w_2(n), \ldots, w_P(n)]^T$, respectively, where, $T$ is transpose operator. In this work, to reduce the computational complexity and to increase the convergence rate, lower order adaptive filter was considered. The following equations are computed recursively until mean square error (MSE) is minimum.

$$\mathbf{a}(n) = \frac{\eta^{-1}\mathbf{B}(n)\mathbf{r}_2(n)}{1 + \eta^{-1}\mathbf{r}_2^T(n)\mathbf{B}(n)\mathbf{r}_2(n)} \tag{1}$$

$$\hat{r}_1(n) = \mathbf{w}^T(n)\mathbf{r}_2(n) \tag{2}$$

$$e(n) = \hat{s}(n) = y(n) - \hat{r}_1(n) \tag{3}$$

$$\mathbf{w}(n+1) = \mathbf{w}(n) + \mathbf{a}(n)e(n) \tag{4}$$

$$\mathbf{B}(n+1) = \eta^{-1}\mathbf{B}(n) - \eta^{-1}\mathbf{a}(n)\mathbf{r}_2^T(n)\mathbf{B}(n) \tag{5}$$

where, $\mathbf{a}(n)$ and $\mathbf{B}(n)$ are the time-varying gain vector and inverse correlation matrix of the tap input vector $\mathbf{r}_2(n)$ and $\eta$ is a forgetting factor set to 0.9999. The initial values for filter coefficient vector and inverse correlation matrices are set to $\mathbf{w}(1) = \mathbf{0}$ and $\mathbf{B}(1) = \delta^{-1}\mathbf{I}$, where, $\delta$ is a positive constant set to $10^{-3}$ and $\mathbf{I}$ is an identity matrix. In order to estimate the EEG signal, first the contaminated EEG signal $y(n) = s(n) + pr_1(n)$ is applied to the primary input of the ANC, where, $s(n)$ and $r_1(n)$ are the $n^{th}$ sample of the desired signal (*i.e*. true EEG) and the artifact or noise signal, respectively and $p$ denote the propagation constant varies with the distance between the EEG electrode placement from the eye and hence decides the amount of EOG artifact buried in the EEG signal. As a second input a signal $r_2(n)$ which is correlated with the $r_1(n)$, is applied to the reference input. As the ANC is able to track the signal changes, after few iterations the estimated $\hat{r}_1(n)$ is approximately equal to $pr_1(n)$ in the primary input signal. Finally, the corrected EEG signal

Authorized licensed use limited to: Universita degli Studi di Roma La Sapienza. Downloaded on October 07,2021 at 15:30:23 UTC from IEEE Xplore. Restrictions apply.

is obtained by subtracting the $\hat{r}_1(n)$ from $y(n)$ in every instant of time $n$, is given by

$$e(n) = y(n) - \hat{r}_1(n) = s(n) + pr_1(n) - \hat{r}_1(n) = \hat{s}(n) \quad (6)$$

### B. Discrete Wavelet Transform

Wavelet transform is a useful tool for analyzing the signals. The advantage of the wavelet transform is that, it can provide the temporal as well as spectral information of the signal, that means, it can provide the better temporal resolution for higher frequency components and better frequency resolution for lower frequency components. Hence the wavelet transform is used for the multi resolution analysis (MRA) of a signal. The given signal, $y(t)$ can be represented into wavelet series as follows [21].

$$y(t) = \sum_m a_{Mm}\phi_{Mm} + \sum_{l=1}^{M}\sum_m d_{lm}\varphi_{lm}(t) \quad (7)$$

where $a_{Mm}$ and $d_{lm}$ are the approximate and detail coefficients respectively. For a given level of decomposition, say $M$, the original signal $y(t)$ can be reconstructed using the approximation and the detail coefficients, as given by

$$y(t) = A_M(t) + \sum_{l=1}^{M} D_l(t) \quad (8)$$

### C. DWT-ANC

In DWT-ANC [20], to construct reference signal *i.e.* EOG signal, needed for ANC, first, using $db4$ mother wavelet and seven decomposition levels, wavelet decomposition is employed on the contaminated EEG signal and obtained approximate and detailed coefficients. Later, soft threshold is applied on lowest three level coefficients and construct the reference signal for ANC by performing the wavelet reconstruction using newly derived wavelet coefficients. Finally, constructed EOG signal is used as reference signal and at the output of the ANC, corrected EEG signal $\hat{s}(n)$ is obtained by subtracting the adaptive filter output from the contaminated EEG signal. Even though DWT-ANC exhibits better performance than the technique proposed in [22], the selection of mother wavelet function and number of decomposition levels depends on the morphology and spectral characteristics of the source of interest. Hence in this paper we proposed a SSA-ANC technique which is independent of morphology of the signal of interest.

## III. Proposed SSA-ANC Methodology to Remove EOG Artifact From EEG Signal

Consider a proposed SSA-ANC based EOG artifact removal system as shown in Fig. 2, that receives the contaminated EEG signal $y(n) = s(n) + pr_1(n)$, with $s(n)$ representing EEG signal and $r_1(n)$ representing the EOG signal and $p$ is the propagation constant which decides the contribution of EOG signal in $y(n)$. As the SSA technique can be operated for block of data, first the incoming data sequence $y(n)$ is stored into buffer of length $N$, results a signal vector

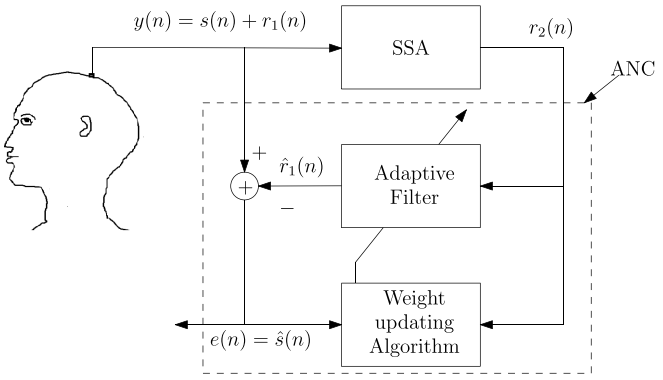


Fig. 2. Block diagram of the proposed SSA-ANC technique.

$\mathbf{y} = [y(1), y(2), \ldots, y(N)]$. After that SSA is applied on the signal vector $\mathbf{y}$ to extract reference signal for the ANC. The following subsections present the key steps in SSA and construction of reference signal for ANC.

### A. Singular Spectrum Analysis

The SSA is a subspace based technique often used for the analysis of climatic and geophysics time series [11], [12]. Basically, SSA consists of four steps: embedding, decomposition, grouping, diagonal averaging and reconstruction. In the embedding step, firstly the single channel contaminated EEG signal vector $\mathbf{y}$ so obtained is mapped into multivariate data matrix by arranging $J$ number of lagged vectors of size $L$, results a trajectory matrix $\mathbf{Y}$ of size $L \times J$.

$$\mathbf{Y} = \begin{bmatrix} y(1) & y(2) & ..... & ..... & y(J) \\ y(2) & y(3) & ..... & ..... & y(J+1) \\ : & : & ..... & ..... & : \\ y(L) & y(L+1) & ..... & ..... & y(N) \end{bmatrix} \quad (9)$$

where $J = N - L + 1$ and $L$ is the window length and is chosen using the condition $i.e.\, L > f_s/f$, where, $f_s$ is the sampling frequency and $f$ is frequency of the signal of interest [14], [23]. It is observed that, all the anti-diagonal elements of the trajectory matrix are same, this type of matrix is called hankel matrix.

In the second step of SSA, using SVD, the trajectory matrix $\mathbf{Y}$ is decomposed into $L$ number of trajectory matrices, $\mathbf{Y}_1, \mathbf{Y}_2, \ldots, \mathbf{Y}_L$. Let eigenvalues and eigenvectors of a covariance matrix $\mathbf{C} = \mathbf{Y}\mathbf{Y}^T$ are denoted as $\lambda_1, \lambda_2, \ldots \lambda_L$ and $\mathbf{v}_1, \mathbf{v}_2, \ldots, \mathbf{v}_L$, respectively. Note that the eigenvalues are arranged in the descending order of their magnitudes $i.e.\, \lambda_1 \geq, \ldots, \geq \lambda_L \geq 0$ and also the corresponding eigenvectors $\mathbf{v}_1, \mathbf{v}_2, \ldots, \mathbf{v}_L$. Then the $i^{th}$ trajectory matrix $\mathbf{Y}_i$ is represented as

$$\mathbf{Y}_i = \sqrt{\lambda_i}\mathbf{v}_i\mathbf{u}_i^T \quad i \in \{1, 2, \ldots, L\} \quad (10)$$

where, $\mathbf{u}_i = \mathbf{Y}^T\mathbf{v}_i/\sqrt{\lambda_i}$. After substitution of $\mathbf{u}_i$ in (10), trajectory matrix $\mathbf{Y}_i$ is represented in terms of eigenvectors of the covariance matrix $\mathbf{C}$ and is given by

$$\mathbf{Y}_i = \mathbf{v}_i\mathbf{v}_i^T\mathbf{Y} \quad (11)$$

The term $\mathbf{v}_i\mathbf{v}_i^T$ in (11) represents the subspace corresponding to the $i^{th}$ component present in given signal vector $\mathbf{y}$.

Authorized licensed use limited to: Universita degli Studi di Roma La Sapienza. Downloaded on October 07,2021 at 15:30:23 UTC from IEEE Xplore. Restrictions apply.

By projecting the trajectory matrix $\mathbf{Y}$ onto that subspace, trajectory matrix for $i^{th}$ signal present in $\mathbf{y}$ is obtained. Using the trajectory matrices $\mathbf{Y}_i$'s, the original trajectory matrix $\mathbf{Y}$ can be reconstructed using

$$\mathbf{Y} = \sum_{i=1}^{L} \mathbf{Y}_i \tag{12}$$

The third and most important step in SSA is grouping the trajectory matrices. The obtained trajectory matrices $\mathbf{Y}_i$ are divided into $d < L$ groups, based on the magnitudes of the eigenvalues. Let $K = \{k_1, \ldots, k_q\}$ represents the indices corresponding to the $q$ eigenvalues of the signal components we are interested in. Then the trajectory matrix for $K^{th}$ group can be represented as $\hat{\mathbf{Y}}_K = \sum_{l=k_1}^{k_q} \mathbf{Y}_l$. In basic SSA, the indices of eigenvalues $i = \{1, 2, \ldots, L\}$ are grouped into $d$ disjoint subsets $i.e.$ $K_1, K_2, \ldots, K_d$, then the trajectory matrix $\mathbf{Y}$ can be represented as

$$\mathbf{Y} = \sum_{m=1}^{d} \hat{\mathbf{Y}}_{K_m} \tag{13}$$

In the final step of SSA, the estimated trajectory matrix of the signal of interest $i.e.$ $\hat{\mathbf{Y}}_I$, where, $I$ represents the indices of the eigenvalues of interested signal component, is mapped into single channel signal. For example, let $\hat{y}_{kj}$ is an element of $k^{th}$ row and $j^{th}$ column of the trajectory matrix $\hat{\mathbf{Y}}_I$, then the $n^{th}$ sample of the signal of interest is obtained by averaging anti-diagonal elements of $\hat{\mathbf{Y}}_I$ over all $k$ and $j$, results a single channel signal.

### B. Extraction of Reference Signal for ANC

The critical step in SSA is identifying the subspace of a signal of interest. In [13], MDL criteria has been proposed to automatically identify subspace of signal. However, such criteria impose constraint that the energy of the signal of interest should be high and is well defined signal. For example, in the EEG signal recorded at frontal electrodes $F_{p_1}$ or $F_{p_2}$ the magnitude of EOG artifact is high and well defined or clearly observable, hence such criteria might work well. But, for some specialized applications such as motor imagery task in BCI, the EEG signals often recorded from $C_3$ and $C_4$ electrode positions, in such case, the contribution of EOG artifact in the measured EEG signal is small as compare with the signal recorded from the frontal electrode positions. This is because of the fact that the placement of the EEG electrode is far from the site of the eye, caused for the generating the EOG signals. So, in such conditions, use of MDL criteria gives false estimation of the signal subspace dimension.

Unlike in local SSA, where the signal subspace is identified based on the magnitudes of the eigenvalues, in the proposed method, we use a novel grouping criteria based on the local mobility of the eigenvector. The local mobility represents the signal complexity measure of eigenvectors, as these representing the frequency components present in the signal. Consider an eigenvector $\mathbf{v} = [v(1), v(2), \ldots, v(L)]$ as a signal vector of $L$ number of samples, then the local mobility $m_f$ [24], can be defined as

$$m_{\mathbf{v}} = \frac{\sqrt{\frac{\sum_{j=1}^{L-1} z^2(j)}{L-1}}}{\sqrt{\frac{\sum_{j=1}^{L} v^2(j)}{L}}} \tag{14}$$

where, $z(j) = v(j) - v(j-1)$ indicates the first order local variation of the signal vector $\mathbf{v}$. As the signal vector $\mathbf{z}$ represents the difference of successive samples in $\mathbf{v}$, for slow time varying signals, for example EOG, the root mean square (RMS) value of $\mathbf{z}$ is small. Here, in order to identify the subspace of EOG signal, first, local mobility of each eigenvector is computed. Later, by setting the threshold, which is selected based on priory information, such as max frequency of EOG signal, the arguments of the corresponding eigenvectors are identified. Once after identifying the eigenvectors representing the EOG signal, corresponding trajectory matrices are estimated by computing equation (11). After adding all the trajectory matrices, representing the EOG signal, the resultant trajectory matrix is mapped into single channel EOG signal vector $\mathbf{r}_2 = [r_2(1), r_2(2), \ldots, r_2(N)]$ is placed in $N$ register buffer and is applied to ANC reference input.

### C. SSA-ANC

In the proposed SSA-ANC, contaminated EEG signal vector $\mathbf{y}$ and the extracted EOG signal vector $\mathbf{r}_2$ are applied to primary and reference inputs of the ANC. Adaptive filter takes the samples of $\mathbf{r}_2$ one by one and estimates $\hat{r}_1(n)$ signal by updating the filter coefficients using RLS algorithm. The estimated $\hat{r}_1(n)$ is subtracted from the contaminated EEG signal $y(n)$ at every time instant $n$, results a corrected EEG signal $\hat{s}(n)$. This process will be repeated for each block of data separately. The time taken to obtain the corrected EEG signal of each block is equal to the sum of the computation times of the serial to parallel convertor, the SSA, parallel to serial convertor and the ANC. Since the computation time to obtain the corrected EEG signal is less than the sampling interval of the EEG signal, the proposed method is practically feasible.

## IV. Results

To validate the performance of proposed SSA-ANC, simulations were performed on synthetic and real life contaminated EEG signal. In both cases, the following mixing model was used

$$y(n) = s(n) + pr_1(n) \tag{15}$$

where, $s(n)$, $r_1(n)$ and $y(n)$ are the true EEG, artifact (EOG) and contaminated EEG signals, respectively. The term $p$ is a propagation constant depends on the distance between the EEG electrode placement from the eye and hence decides the amount of EOG artifact buried in the EEG signal. The signal to nose ratio (SNR) of $y(n)$ is given by

$$SNR = \frac{\frac{1}{N}\sum_{n=1}^{N} s^2(n)}{\frac{1}{N}\sum_{n=1}^{N} pr_1^2(n)} \tag{16}$$

Authorized licensed use limited to: Universita degli Studi di Roma La Sapienza. Downloaded on October 07,2021 at 15:30:23 UTC from IEEE Xplore. Restrictions apply.

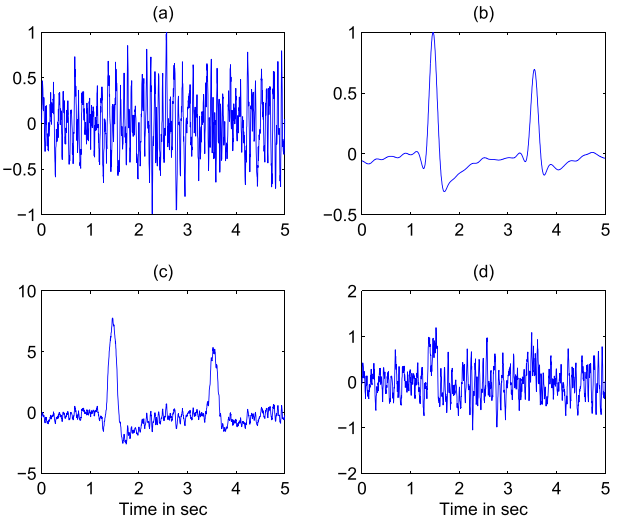


Fig. 3. (a) True EEG signal $s(n)$. (b) EOG signal $r_1(n)$. (c) and (d) Contaminated EEG signal $y(n)$ for $SNR = 0.2$ and 2, respectively.

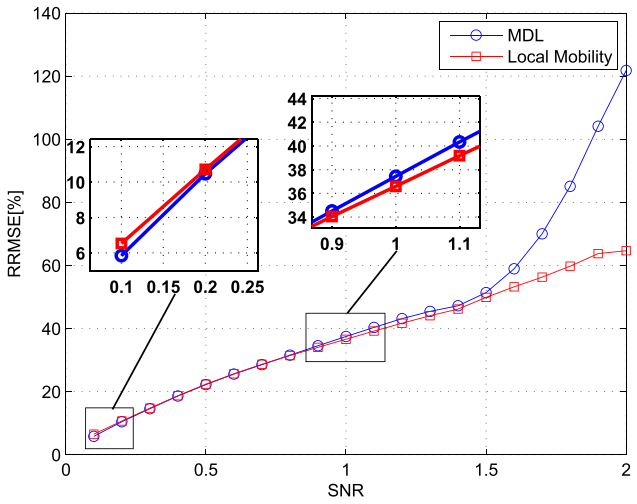


Fig. 4. RRMSE in estimating the EOG artifact using MDL and local mobility criterions.

where, $N$ represent the number of samples. Fig. 3, shows the true EEG signal $s(n)$ and EOG signal $r_1(n)$ as well as synthetically generated contaminated EEG signal $y(n)$ for two different $SNR$ values 0.2 and 2. The synthetic contaminated EEG signal is generated as follows: we have considered a 5 sec of artifact free EEG epoch segmented from $slp32$ polysomnographic record [25], [26]. From a lengthy EOG signal, recorded from one of the author's left eye, a $5sec$ EOG epoch is segmented. Later, we removed high frequency components from the epoch by passing it through a low pass filter of cutoff frequency $5Hz$ and is added to the true EEG segment as per the model given in (15). To quantify the performance of both techniques, relative root mean square error (RRMSE) is used as performance measure and is defined as

$$RRMSE = \frac{RMS(\mathbf{s} - \hat{\mathbf{s}})}{RMS(\mathbf{s})} \times 100\% \tag{17}$$

where, $RMS(\mathbf{s})$ and $RMS(\hat{\mathbf{s}})$ represent the root mean square of true and corrected EEG signals, respectively. In order to achieve better performance, in all the simulations the free parameters, $i.e.$ wavelet function and number decomposition levels, for DWT-ANC, are set to Daubechies4 and seven decomposition levels. The reference signal (EOG) for ANC, is estimated by applying the soft threshold on the low level detailed coefficients ($i.e.$ 3 or 5). In the case of proposed SSA-ANC technique, the window length $L$ is chosen based on the criteria $L > f_s/f$ specified in [14] and [23]. Here, as we are interested in removing the EOG signal, and whose frequency is $<4Hz$, $f$ is set to $3.7Hz$. Thus, window length $L$ is set to 68. Moreover, in order to identify eigenvectors corresponding to the EOG signal, we compute the local mobility $m_f$ of a sinusoidal signal of frequency $3.7Hz$, given $m_f \approx 0.09$, thus threshold is set to 0.1. The reason for selecting sinusoidal signal for setting the threshold is that, as the eigenvectors are oscillating in nature. As the estimated reference signal and artifact in the EEG signal have high similarity, adaptive filter length $P$ is set to one, which intern reduces the computational complexity and increases the convergence rate [20]. The simulation results shows that even if adaptive filter order increases the performance improvement is marginal.

### A. Comparative Study of MDL and Proposed Local Mobility Criterions

To evaluate the comparative study of both MDL and local mobility criterions, we consider the mixing model given in (15). Using the MDL and the local mobility criterions as a grouping techniques, SSA is applied on the single channel contaminated EEG signal and estimate the EOG artifact. The relative root mean square error (RRMSE) obtained in estimating the EOG artifact present in the measured EEG signal using MDL and local mobility criterions is shown in Fig. 4. It is observed from Fig. 4 that for the lower SNRs (0.1), where the EOG artifact is high in magnitude, the MDL criteria is better than the proposed local mobility criteria (shown as subplot in Fig. 4). This is due to the fact that the magnitude of the eigenvalues associated to the EOG artifact are well clustered from the eigenvalues associated to the EEG signal. Hence, the MDL criteria is able to find the EOG artifact subspace efficiently.

However, for higher SNRs ($\geq$1), for example the EEG signals recorded at central electrodes $i.e.$ $C_3$ and $C_4$, the contribution of EOG artifact is small in magnitude and so the magnitudes of the eigenvalues associated to the EOG and EEG signals are not well clustered. Hence, the MDL criteria fails to find the subspace of the EOG artifact for higher SNRs. In general as the EOG signal is a slowly time varying signal, the numerator quantity in (14) is small. Thus, the local mobility of the eigenvectors associated to the EOG artifact is small as compared with the local mobility of the eigenvectors associated with the EEG signal. Hence, the proposed local mobility criteria shows better performance than the MDL criteria for higher SNRs.

### B. Simulation Results Using Synthetic EEG Signals

With the above parameter settings, DWT-ANC, proposed SSA without ANC and proposed SSA with ANC techniques

Authorized licensed use limited to: Universita degli Studi di Roma La Sapienza. Downloaded on October 07,2021 at 15:30:23 UTC from IEEE Xplore. Restrictions apply.

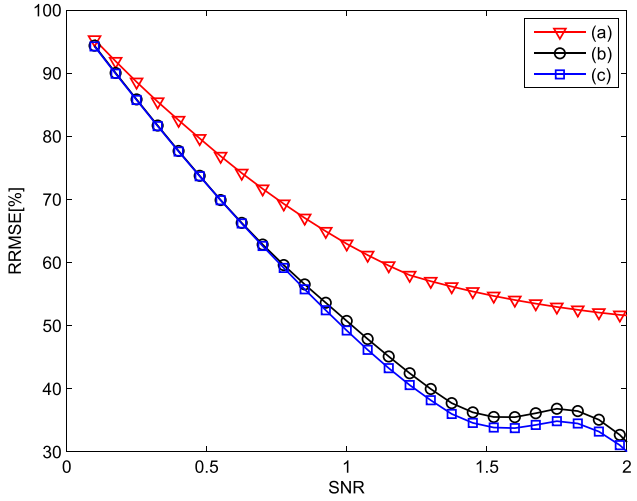


Fig. 5. RRMSE curves for corrected EEG signals using (a) DWT-ANC, (b) proposed SSA without ANC and (c) proposed SSA-ANC techniques, respectively.

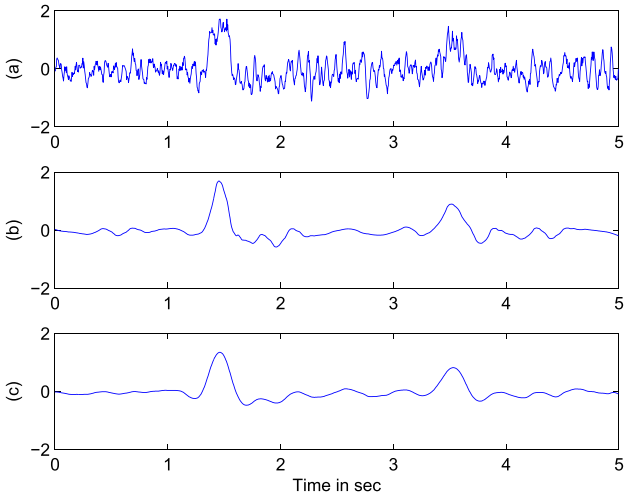


Fig. 6. (a) Synthetic contaminated EEG signal $y(n)$ for $SNR = 1$. (b) Extracted reference signals for ANC using DWT. (c) Extracted reference signal for ANC using SSA.

are applied on synthetically contaminated EEG signal for different $SNRs$. The RRMSE curves for the corrected EEG signals using the DWT-ANC, proposed SSA without ANC and proposed SSA-ANC techniques as a function of $SNR$ are shown in Fig. 5. It is clear from the Fig. 5 that in terms of RRMSE the proposed SSA-ANC gives superior performance than the DWT-ANC and proposed SSA without ANC for different SNRs. It is clear from the Fig. 5 that for higher SNRs ($\geq$1) it is found that introduction of ANC enables a reduction in RRMSE by 1.5% compared to SSA alone and 22% compared to the DWT-ANC. As the proposed SSA-ANC exhibits superior performance than SSA alone, in the subsequent simulations, the performance comparison of proposed SSA-ANC is made with DWT-ANC. Fig. 6 shows the estimated reference signals by DWT and SSA decomposition techniques from the contaminated EEG signal for $SNR = 1$. From Fig. 6 it is observed that the reference signal estimated by DWT has EEG components also, whereas

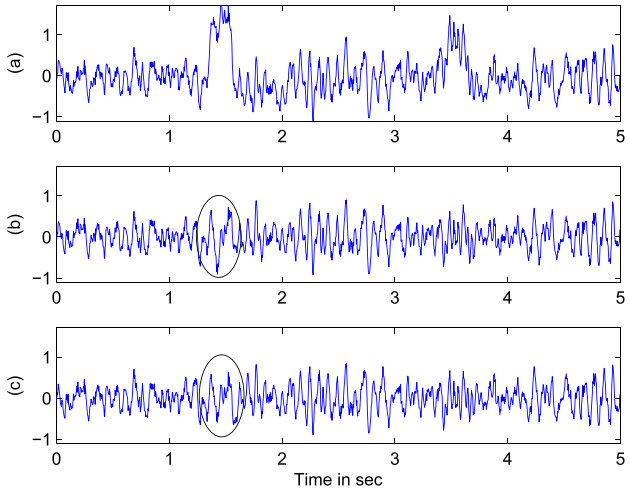


Fig. 7. (a) Synthetically contaminated EEG signal $y(n)$ for $SNR = 1$. (b) Corrected EEG signal by the DWT-ANC. (c) Corrected EEG signal by the proposed SSA-ANC.

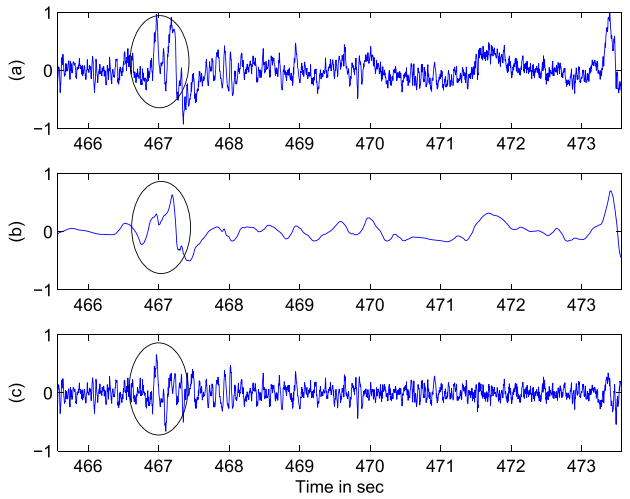


Fig. 8. (a) Contaminated EEG signal. (b) Estimated reference signal for ANC using DWT. (c) Corrected EEG signal by DWT-ANC.

SSA effectively estimate the reference signal without altering the EEG components. This can be observed in the reference signals as smooth base line in the artifact free time zones as compare with the reference signal estimated by DWT. The corrected EEG signals by DWT-ANC and proposed SSA-ANC techniques are shown in Fig. 7. It is clear from encircled portion of Fig. 7 (b) that the corrected EEG signal by DWT-ANC technique is deviates from the EEG signal. This is because of the mother wavelet function. But, the proposed SSA-ANC technique extract the EEG signal efficiently.

### C. Simulation Results Using Real Life EEG Signals

To assess the efficacy of proposed SSA-ANC technique on the real life contaminated EEG signals, we consider EEG data recorded for BCI motor imagery study [27]–[29]. As this data is recorded for movement imagery task, there will be a $\alpha$ $(8 - 12Hz)$ component present in the measured EEG signal. To evaluate the proposed SSA-ANC technique on this data, 8 sec of EEG epoch contaminated by EOG artifact is considered. Fig. 8. shows the estimated EOG reference signal and corrected EEG signal by DWT-ANC. It is noticed from

Authorized licensed use limited to: Universita degli Studi di Roma La Sapienza. Downloaded on October 07,2021 at 15:30:23 UTC from IEEE Xplore. Restrictions apply.

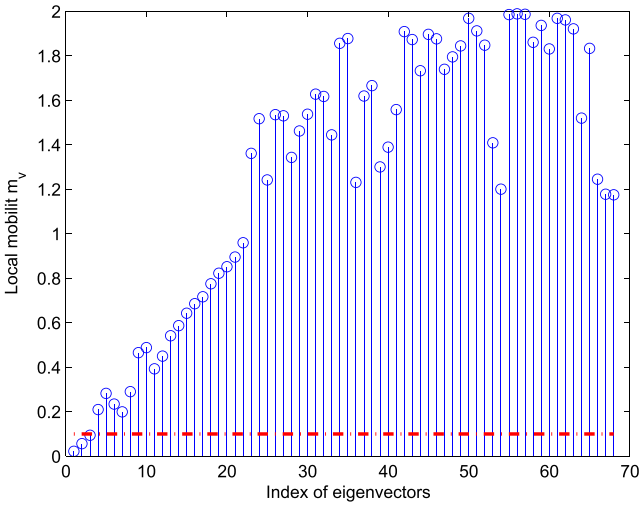


Fig. 9. Local mobilities of eigenvectors for window length $L = 68$.

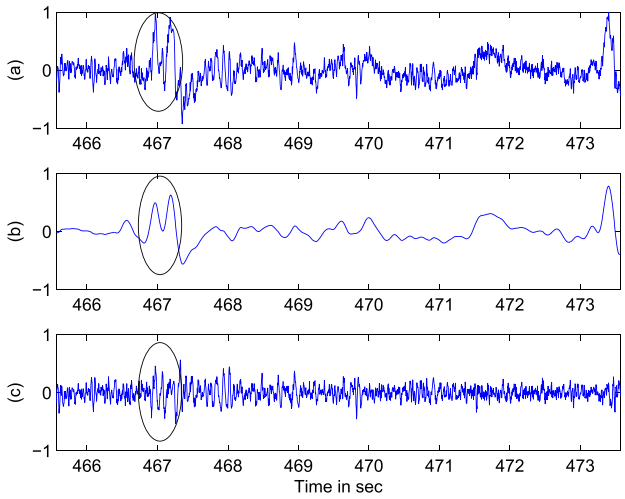


Fig. 10. (a) Contaminated EEG signal. (b) estimated reference signal for ANC using SSA. (c) Corrected EEG signal by proposed SSA-ANC.

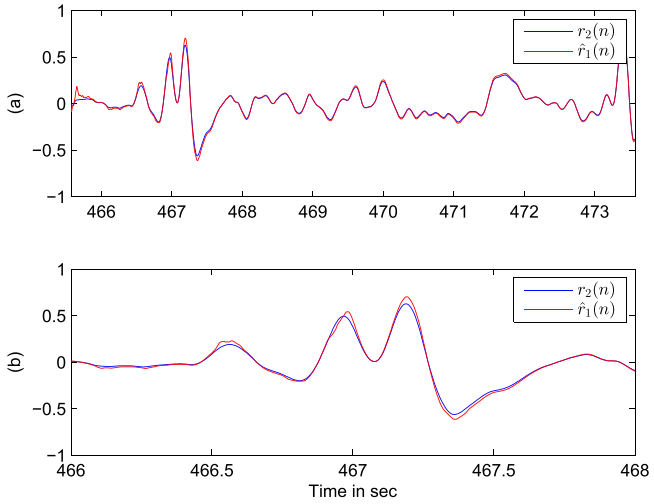


Fig. 11. (a) Estimated EOG reference signal by SSA $\mathbf{r}_2(n)$ and adaptive filter output $\hat{r}_1(n)$. (b) Zoomed version of above plot between time interval 466 to 468$sec$.

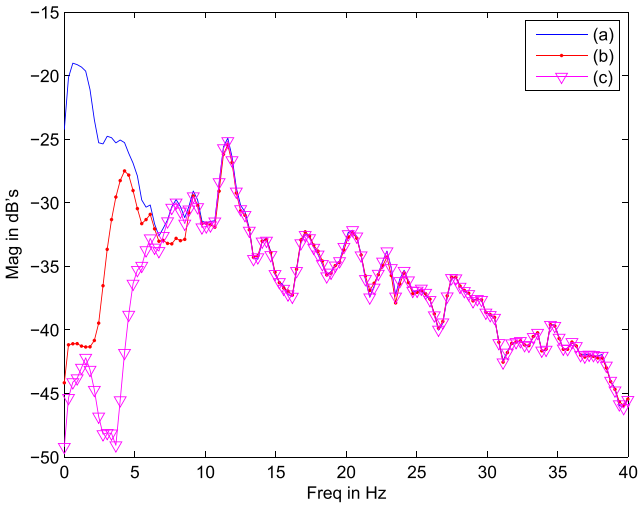


Fig. 12. PSD of (a) contaminated EEG signal, (b) corrected EEG signal by DWT-ANC and (c) corrected EEG signal by SSA-ANC.

Fig. 8(b)-(c) that the reference and corrected EEG signals using DWT-ANC are poorly reconstructed, shown in circle. The reason is that the morphologies of the wavelet function and eye blink at that instant are not matched. From these results it is noted that the performance of the DWT-ANC is depends on the selection of mother wavelet function. In the proposed SSA-ANC technique, after performing first two steps of SSA, local mobility of each eigenvector is computed. Fig. 9 shows the local mobility of each eigenvector and dotted line indicates the threshold 0.1. From Fig. 9 it is found that eigenvectors $\mathbf{v}_1, \mathbf{v}_2$ and $\mathbf{v}_3$ are the basis vectors to construct the EOG signal (reference) for ANC. The reconstructed reference and corrected EEG signals using proposed SSA-ANC technique are shown in Fig. 10. Comparing the reference signals obtained by DWT-ANC (Fig. 8(b)) and proposed SSA-ANC (Fig. 10(b)), SSA outperforms in reconstructing the EOG signal than the DWT. In conventional methods, the extracted EOG signal is simply subtracted from the contaminated EEG to obtained artifact free EEG signal. However, this technique fails to track the signal changes due to the eye blink. Hence use of ANC enhance in the process of estimating EOG artifact. Fig 11(a) shows the reconstructed EOG signals at output of SSA and adaptive filter blocks. The improvement in the estimated EOG signal can be clearly observed in Fig. 11(b). From the above simulations it is concluded that, unlike DWT-ANC, where the performance is depends on the morphology of the EOG artifact, the proposed SSA-ANC performance does not depend on the morphology of the EOG signal, hence is a suitable candidate for the removal of EOG artifact from the EEG signal. The efficiency of the proposed SSA-ANC technique in removing the EOG artifact can be observed from the power spectral density (PSD) of the contaminated and corrected EEG signals, shown in Fig. 12. It is clear from Fig. 12 that the proposed SSA-ANC technique efficiently attenuate the EOG signal and is justified as small power in frequency band $0.5 - 4Hz$ than the PSD of the corrected EEG signal by DWT-ANC. In order to show that the proposed SSA-ANC technique is preserves

Authorized licensed use limited to: Universita degli Studi di Roma La Sapienza. Downloaded on October 07,2021 at 15:30:23 UTC from IEEE Xplore. Restrictions apply.

TABLE I
MEAN ABSOLUTE ERROR (MAE) OF TWO TECHNIQUES

| Segment | DWT-ANC (dB) | Proposed SSA-ANC (dB) |
|---|---|---|
| 1 | 0.4382 | 0.1949 |
| 2 | 0.7456 | 0.2072 |
| 3 | 0.2440 | 0.2152 |
| 4 | 0.1057 | 0.0980 |
| 5 | 0.5501 | 0.1206 |
| Average | 0.4167 | 0.1671 |

the EEG $\alpha$ component, we define a parameter called, mean absolute error (MAE) and is given by

$$MAE = \frac{\sum_{k=j}^{l} \mid \mathbf{p}_e(k) - \mathbf{p}_y(k) \mid}{l - j} \tag{18}$$

where, $\mathbf{p}_e$ and $\mathbf{p}_y$ are the PSD of the corrected and contaminated EEG signals respectively and $j$ and $l$ are the specific frequency bands. First, we applied DWT-ANC and proposed SSA-ANC techniques on the five EEG epochs which are fully contaminated by EOG artifacts and compute the PSDs of contaminated and corrected EEG signals. Later MAE for the EEG $\alpha$ band $10-12Hz$ is computed. Table I shows the MAE for both techniques and is showed that on average MAE for proposed SSA-ANC results $0.1671dB$ error, which is smaller than the DWT-ANC. Hence we can conclude that proposed SSA-ANC technique is not altering the EEG $\alpha$ component.

## V. CONCLUSION

In this paper, combined SSA and ANC technique is presented to remove the EOG artifacts from the single channel EEG signals. In this technique, the reference signal (EOG) for ANC is extracted using SSA, thus avoids the use of separate electrodes to record EOG signal. More importantly, unlike DWT-ANC, where the performance is depends on the morphology of the EOG artifact, the proposed SSA-ANC performance is independent of the morphology of the EOG signal, hence better performance is achieved by proposed SSA-ANC. The simulation results also demonstrate the efficiency of the proposed SSA-ANC over DWT-ANC in terms of RRMSE and MAE. As the proposed SSA-ANC technique is able to operate on single channel EEG signals, this can be applicable for portable applications.

## ACKNOWLEDGMENT

The authors would like to thank the anonymous reviewers whose comments and suggestions helped to enhance the quality of this paper.

## REFERENCES

[1] M. Fatourechi, A. Bashashati, R. K. Ward, and G. E. Birch, "EMG and EOG artifacts in brain computer interface systems: A survey," *Clin. Neurophysiol.*, vol. 118, no. 3, pp. 480–494, 2007.
[2] R. Verleger, T. Gasser, and J. Möcks, "Correction of EOG artifacts in event-related potentials of the EEG: Aspects of reliability and validity," *Psychophysiology*, vol. 19, no. 4, pp. 472–480, 1982.
[3] J. C. Woestenburg, M. N. Verbaten, and J. L. Slangen, "The removal of the eye-movement artifact from the EEG by regression analysis in the frequency domain," *Biol. Psychol.*, vol. 16, nos. 1–2, pp. 127–147, 1983.
[4] S. Haykin, *Adaptive Filter Theory*. Pearson Education India, 2008.
[5] B. Widrow *et al.*, "Adaptive noise cancelling: Principles and applications," *Proc. IEEE*, vol. 63, no. 12, pp. 1692–1716, Dec. 1975.
[6] W. Du, H. M. Leong, and A. S. Gevins, "Ocular artifact minimization by adaptive filtering," in *Proc. IEEE 7th SP Workshop Statist. Signal Array Process.*, Jun. 1994, pp. 433–436.
[7] P. He, G. Wilson, and C. Russell, "Removal of ocular artifacts from electro-encephalogram by adaptive filtering," *Med. Biol. Eng. Comput.*, vol. 42, no. 3, pp. 407–412, 2004.
[8] M. Z. U. Rahman, R. A. Shaik, and D. V. R. K. Reddy, "Efficient and simplified adaptive noise cancelers for ECG sensor based remote health monitoring," *IEEE Sensors J.*, vol. 12, no. 3, pp. 566–573, Mar. 2012.
[9] G. V. S. Karthik, S. Y. Fathima, M. Z. U. Rahman, S. R. Ahamed, and A. Lay-Ekuakille, "Efficient signal conditioning techniques for brain activity in remote health monitoring network," *IEEE Sensors J.*, vol. 13, no. 9, pp. 3276–3283, Sep. 2013.
[10] C. Guerrero-Mosquera and A. Navia-Vázquez, "Automatic removal of ocular artefacts using adaptive filtering and independent component analysis for electroencephalogram data," *IET Signal Process.*, vol. 6, no. 2, pp. 99–106, Apr. 2012.
[11] M. Ghil *et al.*, "Advanced spectral methods for climatic time series," *Rev. Geophys.*, vol. 40, no. 1, pp. 1–41, Sep. 2002.
[12] N. Golyandina, V. Nekrutkin, and A. A. Zhigljavsky, *Analysis of Time Series Structure: SSA and Related Techniques* (Monographs on statistics and applied probability), vol. 90. Boca Raton, FL, USA: Chapman & Hall, 2001.
[13] A. R. Teixeira, A. M. Tomé, E. W. Lang, P. Gruber, and A. M. da Silva, "On the use of clustering and local singular spectrum analysis to remove ocular artifacts from electroencephalograms," in *Proc. IEEE Int. Joint Conf. Neural Netw. (IJCNN)*, vol. 4, Jul. 2005, pp. 2514–2519.
[14] A. R. Teixeira, A. M. Tomé, E. W. Lang, P. Gruber, and A. M. da Silva, "Automatic removal of high-amplitude artefacts from single-channel electroencephalograms," *Comput. Methods Programs Biomed.*, vol. 83, no. 2, pp. 125–138, Aug. 2006.
[15] C. M. Bishop, *Neural Networks for Pattern Recognition*. New York, NY, USA: Oxford Univ. Press, 1995.
[16] A. P. Liavas and P. A. Regalia, "On the behavior of information theoretic criteria for model order selection," *IEEE Trans. Signal Process.*, vol. 49, no. 8, pp. 1689–1695, Aug. 2001.
[17] G. Pfurtscheller and F. H. L. da Silva, "Event-related EEG/MEG synchronization and desynchronization: Basic principles," *Clin. Neurophysiol.*, vol. 110, no. 11, pp. 1842–1857, 1999.
[18] W. Yi, S. Qiu, H. Qi, L. Zhang, B. Wan, and D. Ming, "EEG feature comparison and classification of simple and compound limb motor imagery," *J. Neuroeng. Rehabil.*, vol. 10, p. 106, Oct. 2013.
[19] S. Sanei, T. K. M. Lee, and V. Abolghasemi, "A new adaptive line enhancer based on singular spectrum analysis," *IEEE Trans. Biomed. Eng.*, vol. 59, no. 2, pp. 428–434, Feb. 2012.
[20] H. Peng *et al.*, "Removal of ocular artifacts in EEG—An improved approach combining DWT and ANC for portable applications," *IEEE J. Biomed. Health Informat.*, vol. 17, no. 3, pp. 600–607, May 2013.
[21] B. Azzerboni, M. Carpentieri, F. La Foresta, and F. C. Morabito, "Neural-ICA and wavelet transform for artifacts removal in surface EMG," in *Proc. IEEE Int. Joint Conf. Neural Netw.*, vol. 4, Jul. 2004, pp. 3223–3228.
[22] H. Peng, B. Hu, Y. Qi, Q. Zhao, and M. Ratcliffe, "An improved EEG de-noising approach in electroencephalogram (EEG) for home care," in *Proc. 5th Int. Conf. Pervasive Comput. Technol. Healthcare (PervasiveHealth)*, May 2011, pp. 469–474.
[23] C. J. James and D. Lowe, "Extracting multisource brain activity from a single electromagnetic channel," *Artif. Intell. Med.*, vol. 28, no. 1, pp. 89–104, 2003. [Online]. Available: http://www.sciencedirect.com/science/article/pii/S093336570300037X
[24] K. Najarian and R. Splinter, *Biomedical Signal and Image Processing*. Boca Raton, FL, USA: CRC Press, 2005.
[25] Y. Ichimaru and G. B. Moody, "Development of the polysomnographic database on CD-ROM," *Psychiatry Clin. Neurosci.*, vol. 53, no. 2, pp. 175–177, 1999.
[26] A. L. Goldberger *et al.*, "PhysioBank, PhysioToolkit, and PhysioNet: Components of a new research resource for complex physiologic signals," *Circulation*, vol. 101, no. 23, pp. e215–e220, Jun. 2000.
[27] M. Tangermann *et al.*, "Review of the BCI competition IV," *Frontiers Neurosci.*, vol. 6, no. 55, p. 2, 2012.
[28] M. Naeem, C. Brunner, R. Leeb, B. Graimann, and G. Pfurtscheller, "Seperability of four-class motor imagery data using independent components analysis," *J. Neural Eng.*, vol. 3, no. 3, p. 208, 2006.
[29] A. Schlögl, C. Keinrath, D. Zimmermann, R. Scherer, R. Leeb, and G. Pfurtscheller, "A fully automated correction method of EOG artifacts in EEG recordings," *Clin. Neurophys.*, vol. 118, no. 1, pp. 98–104, 2007.

Authorized licensed use limited to: Universita degli Studi di Roma La Sapienza. Downloaded on October 07,2021 at 15:30:23 UTC from IEEE Xplore. Restrictions apply.

**Ajay Kumar Maddirala** received the B.Tech. degree in electronics and communication engineering from Jawaharlal Nehru Technological University, Hyderabad, India, in 2005, and the M.Tech. degree in electronics and communication engineering from Jawaharlal Nehru Technological University, Kakinada, India, in 2010. He is currently pursuing the Ph.D. degree with the Indian Institute of Technology Guwahati, India.

He was a Lecturer with Sri Prakash College of Engineering, Tuni, India, from 2006 to 2007. From 2010 to 2011, he was an Assistant Professor with Narasaraopet Engineering College, Narasaraopet, India. His research interests include biomedical signal processing and adaptive signal processing.

**Rafi Ahamed Shaik** received the B.Tech. and M.Tech. degrees in electronics and communication engineering from Sri Venkateswara University, Tirupati, India, in 1991 and 1993, respectively, and the Ph.D. degree from the Indian Institute of Technology Khargpur, India, in 2008. He is currently an Associate Professor with the Department of Electronics and Communication Engineering, Indian Institute of Technology Guwahati, Guwahati, India.

He was a Faculty Member with the Deccan College of Engineering and Technology, Hyderabad, India, from 1993 to 1995, and Bapatla Engineering College, Bapatla, India, from 1995 to 2003. His teaching and research interests are in digital and adaptive signal processing, biomedical signal processing, and VLSI signal processing.

Authorized licensed use limited to: Universita degli Studi di Roma La Sapienza. Downloaded on October 07,2021 at 15:30:23 UTC from IEEE Xplore. Restrictions apply.